Electronic Supplementary Material (ESI) for Nanoscale

Electronic Supplementary Information for GHz operation of nanometer-scale metallic Ag2S memristors

Attila Geresdi, Miklós Csontos,* Agnes Gubicza, András Halbritter, and György Mihály
Department of Physics, Budapest University of Technology and Economics and Condensed Matter Research Group of the Hungarian Academy of Sciences, Budafoki ut 8, 1111 Budapest, Hungary

Ag thin films with a nominal thickness of 80 nm were vacuum evaporated onto a Si substrate. The thin Ag_2S layers were grown by depositing sulfur onto the Ag surfaces in a clean environment. First, analytic grade sulfur powder was loaded in a quartz tube, melted and cooled back in order to ensure a homogenous source. The thin film sample was then loaded in the tube to a distance of 2 cm from the sulfur. After loading both the sulfur and the sample, the tube was evacuated to 10^{-5} mbar pressure. Then the temperature was ramped up to 60 °C and the sublimation of the sulfur was performed in a static vacuum for 2–10 minutes. Finally, the temperature was rapidly ramped down.

The samples were characterized by He-RBS (Rutherford Backscattering Spectrometry) and ERDA (Elastic Recoil Detection Analysis) [1]. They exhibit inhomogeneous sulfur concentration profiles consistent with the presence of an Ag_2S surface layer [2].

Nanoscale contacts were created by gently touching the sample surface with a mechanically sharpened PtIr or Nb tip. For coarse adjustment a screw thread mechanism was used, whereas for the fine positioning a three dimensional piezo scanner was applied. Using this technique numerous contacts were created with reproducible I-V characteristics. The bias voltage was applied to the junctions by utilizing the analog outputs of a National Instruments data acquisition card. The output voltage was divided and filtered in order to ensure low noise on the contact. The current was measured using a variable range I-V converter and processed by the data acquisition card. The current-voltage characteristics of the junctions were recorded during repeated bias voltage sweeps.

The bias scheme of the I-V measurements carried out with a superconducting Nb tip at 4.2 K is shown in Fig. S1(a). The subsequent resistive switchings are obtained by voltage sweeps of 800 mV amplitude and alternating sign while the ON and OFF state resistances as well as the non-linear current contributions induced by the superconducting tip are detected by low amplitude (± 10 mV) triangular voltage pulses. The first high bias sweep is performed in order to verify the switching and to initialize the device in its OFF state. This is followed by the acquisition of the low bias IV data repeated 5 times for averaging purposes in order to further improve the signal to noise ratio. The next high bias sweep covers one and a half of the total hysteresis loop preparing the device in its ON state before the second sequence of the low bias measurements probing the ON state transport properties are executed. In order to confirm that upon the first OFF to ON switching and ON state measurements the device preserved its reversible configuration, we restored and tested the OFF state again by applying another high bias loop and a low bias sequence, respectively. The reproducibility of the hysteretic high bias I-V traces shown in Fig. S1(b) demonstrate that the two dominant device configurations determining the ON and OFF states did not change over the above sweeping sequences. Fitting the numerical derivative of the low bias I-V data displayed in Fig. S1(c) against the BTK theory provides information about the effective transmission values of the corresponding configurations.

The numerical accuracy of the fitting procedure on T is illustrated in Fig. S2. After obtaining the best fitting transmission values by a numerical least square method, T was detuned from its optimum to the values indicated

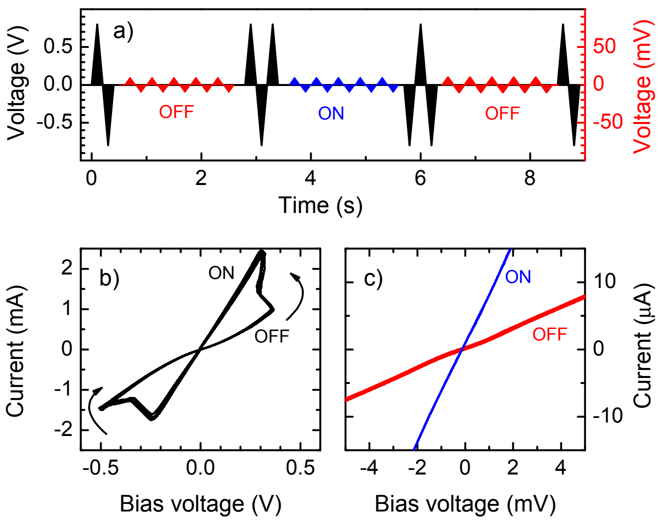

FIG. S1. (a) Biasing scheme of the I-V measurements. The 800 mV amplitude voltage sweeps (black triangles) are used to record the hysteretic switching characteristics and to prepare the subsequent OFF/ON/OFF states for the voltage sweeps performed repeatedly on the scale of the Nb superconducting gap between ± 10 mV (red and blue triangles). (b) Hysteretic high bias I-V characteristics of an Ag-Ag_2S sample and a superconducting Nb tip. The overlap of the 4 subsequent loops demonstrate reproducible resistive switching over the entire pulsing sequence. The arrows indicate the direction of the bias sweep. (c) Low bias I-V traces corresponding to the ON (1 trace) and OFF states (2 overlapping traces). All data were taken at 4.2 K.

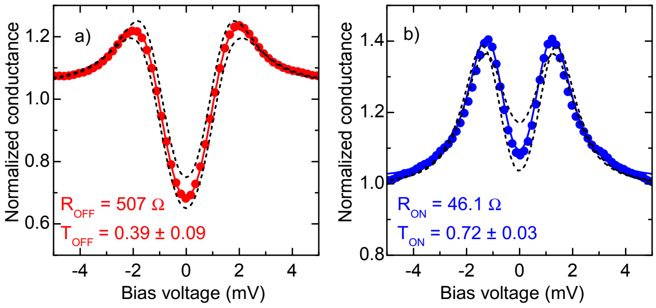

FIG. S2. Representative finite bias conductance in the OFF (a) and ON states (b) of an Ag-Ag_2S-Nb junction at 4.2 K obtained by numerical differentiation of the measured low bias I-V traces. Continuous lines denote fits using the BTK theory with the obtained transmission values shown in the graphs. Note that each curve is normalized to its high bias ($eV \gg \Delta = 1.4$ meV) value $G_{\mathrm{ON,OFF}} = (R_{\mathrm{ON,OFF}})^{-1}$. The dashed lines correspond to the best fits using the detuned transmission values as labeled in the graphs testifying to the accuracy of our analysis on T.

in Fig. S2. The fitting procedure was repeated with the broadening parameter Γ and the superconducting gap Δ as the remaining free parameters while the temperature and the normal state conductance were kept at their pre-determined values. The best fitting curves obtained by this procedure are displayed by dashed lines in Fig. S2. Their systematic deviation from the experimental data demonstrates that the nominated $\Delta T_{\mathrm{OFF}}/T_{\mathrm{OFF}} = 0.20$ and $\Delta T_{\mathrm{ON}}/T_{\mathrm{ON}} = 0.05$ relative errors indeed represent a lower limit on the accuracy of the transmission values determined by the modified BTK model. While the former seems to be a rather conservative estimate, the metallic nature of the OFF states is still evident. Consequently, our attempts to fit the individual differential conductance traces by the parallel contributions of a small, highly transparent channel and a poorly transmitting but extended area junction, the latter dominating G_N, have systematically failed.

The pulsing scheme along with the circuit layout utilized in the room temperature sub-nanosecond pulsing experiments is shown in Fig. S3. The setup is based on a custom built rise time avalanche pulse generator relying on the periodic charging (break-down) of the bipolar transistor indicated in Fig. S3(a) through a 1 MΩ resistor and a 2 pF capacitor (50 Ω resistor) yielding to unipolar outbursts specified to a 500 ps pulse width and ∼10 V amplitude at a repetition rate of ∼500 kHz [3]. In order to study the resistive switching behavior of our memristor samples in this unipolar pulsing configuration, the device has to be re-initialized in its OFF state in each cycle of the pulsing sequence by applying a sufficiently large negative bias. The read-out is performed at low negative bias levels applied before and after the short pulses. These slow, typically 50 μs long signals are added to the bias-

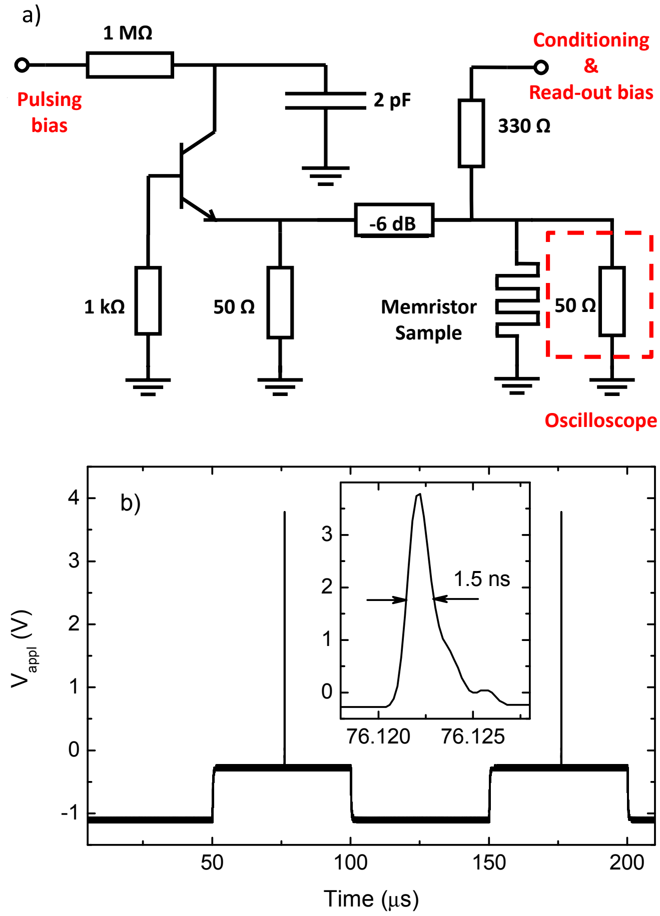

FIG. S3. (a) The circuit layout of the room temperature setup utilized to apply a high (low) negative conditioning (read-out) bias and short voltage pulses of 500 ps duration on the memristor sample. (b) The applied pulsing sequence as recorded in an open circuit configuration. The sample is initialized in its OFF state by the application of the 50 μs long conditioning pulses of -1.1 V amplitude while the 50 μs long read-out pulses of -300 mV amplitude are used to determine the status of the device before and after the short pulses. The apparent 1.5 ns width of the nominally 500 ps pulses (inset) is the consequence of the limited, 250 MHz oscilloscope bandwidth.

ing circuit via the dc terminal shown in the right hand side of the layout in Fig. S3(a). In order to gain control on the timing of the 500 ps pulses, the onset of the read-out signal is used to gate the 75 V dc bias of the pulse generator. The voltage drop on the memristor sample is monitored by a digital oscilloscope with an effective time resolution of 2 ns. The pulsing sequence shown in Fig. S3(b) was recorded in an open circuit configuration, i.e. when the memristor device is replaced by an open terminal, exhibiting transient behavior decaying within 3 ns after the fall of the short pulses.

* csontos@dept.phy.bme.hu

[1] E. Kótai, Nucl. Instrum. Methods B **85**, 588 (1994).
[2] A. Geresdi, A. Halbritter, E. Szilágyi, and G. Mihály, MRS Proceedings **1331** (2011).
[3] J. Williams, *Linear Technology Application Note*, vol. 47 (1991), URL `http://cds.linear.com`.